General Disclaimer

One or more of the Following Statements may affect this Document

- This document has been reproduced from the best copy furnished by the organizational source. It is being released in the interest of making available as much information as possible.

- This document may contain data, which exceeds the sheet parameters. It was furnished in this condition by the organizational source and is the best copy available.

- This document may contain tone-on-tone or color graphs, charts and/or pictures, which have been reproduced in black and white.

- This document is paginated as submitted by the original source.

- Portions of this document are not fully legible due to the historical nature of some of the material. However, it is the best reproduction available from the original submission.

NASA TECHNICAL MEMORANDUM

NASA TM X-71819

(NASA-TM-X-71819) CN THE EFFECTS OF FLIGHT
ON JET ENGINE EXHAUST NOISE (NASA) 26 p HC
$4.00   CSCL 20A

N76-12066

G3/07   Unclas
         02992

ON THE EFFECTS OF FLIGHT ON
JET ENGINE EXHAUST NOISE

by James R. Stone
Lewis Research Center
Cleveland, Ohio 44135

ON THE EFFECTS OF FLIGHT ON JET ENGINE EXHAUST NOISE

by James R. Stone

Lewis Research Center

ABSTRACT

Recent flight data on jet engine exhaust noise do not agree with pro-
jections based on classical jet noise theories. This paper demonstrates
that these differences may be reconciled by considering the combined ef-
fects of jet mixing noise and internally-generated engine exhaust noise.
The source strength of the internally-generated noise is assumed to be
unaffected by flight, as has been shown in small-scale free-jet experi-
ments. The directivity of the internally-generated noise is assumed to
be the same statically as that given in the NASA interim prediction method
for core engine noise. However, it is assumed that in flight the internally
generated noise is subject to the convective amplification effect of a simple
source. The absolute levels of the internally-generated noise are obtained
from an empirical fit of some typical engine data. The static and flight jet
noise are predicted using the NASA interim prediction method for jet noise.
It is shown that in many cases, although jet mixing may be the dominant
noise source statically, much of the flyover noise signature is dominated
by internally-generated noise.

INTRODUCTION

To assess the environmental impact of aircraft noise it is necessary
to predict the effect of flight on jet engine exhaust noise. For new or pro-
posed airplanes particularly, such predictions will be based at least in part
on model and full-scale static and simulated-flight tests. Because of costs,
to rely solely on full-scale flight tests would severely limit the number of
configurations and concepts that could be tested. Therefore, it is essential
to be able to predict flight noise from static or simulated-flight data.

Early noise prediction methods (e.g., ref. 1) assumed that jet noise is simply a function of relative jet velocity, $V_j - V_o$. (All symbols are defined in the appendix.) Consequently, jet mixing noise should be attenuated in flight. Ffowcs Williams (ref. 2) has obtained a slightly different result by modifying Lighthill's jet noise theory (refs. 3 and 4) to account for the fact that the noise generating turbulent eddies move relative to both the moving aircraft and the observer. This analysis (ref. 2) indicates that for a subsonic jet the intensity of the noise is a function of relative velocity to the seventh power multiplied by jet velocity, $(V_j - V_o)^7 V_j$. Alternatively, this result can be restated as follows: with increasing forward velocity the reduction in overall sound pressure level (OASPL) relative to static conditions at the same jet velocity is given by $10 \log (1 - V_o/V_j)^n$, where in this case $n = 7$. Tests of small jets in large, free-jet, flight-simulation facilities (refs. 5 to 7) have indicated a smaller effect of forward velocity, i.e. $n \leqq 6$. Somewhat similar results have been reported in reference 8 for tests in an acoustic wind tunnel. The results of reference 5 have been incorporated into a general prediction of jet noise in reference 9.

Recent flight data (e.g., refs. 10 and 11) on jet engine exhaust noise do not agree with projections from static data based on the effects discussed in the preceding paragraph for jet noise. Figure 1 is typical of these results (ref. 10), the OASPL directivity is plotted for level flyovers of the HS 125 airplane powered by the Viper 601 turbojet engine. Static data for this engine, extrapolated to the same distance for comparison, are also shown. It can be seen that the in-flight noise levels are actually higher than the static levels over a wide range of directivity angles. It is the purpose of this paper to demonstrate that these apparently anomalous flight effects can be reconciled largely on the basis of the combined contributions of jet mixing noise and internally-generated exhaust noise.

In the present report, initially, measured jet mixing and internal noise static data are compared with prediction methods to establish the validity of the latter. Due to the lack of component noise data for most flight tests, the effect of flight on jet engine exhaust noise is then assessed by means of

the prediction methods. Static and in-flight jet engine exhaust noise levels are computed based primarily on the NASA interim noise prediction methods (refs. 9 and 12). The absolute levels of the internally-generated noise are obtained from an empirical fit of some engine static data from reference 13. The jet noise is predicted, statically and in flight, by the methods of reference 9. The source strength of the internally-generated noise is assumed to be unaffected by flight, as has been shown in small-scale free jet experiments (ref. 14). The directivity of the internally-generated noise is assumed to be the same statically as that given for engine core noise in references 12 and 15. It is assumed that in flight the internally-generated noise is subject to the convective amplification of a simple noise source, $-40 \log (1 - M_0 \cos \theta)$ (refs. 16 - 18). Finally, the sensitivity of the results to the specific assumptions made is also considered.

PREDICTION METHODS

It will be shown in this report that the noise of a jet engine in flight, in the absence of dominant fan and compressor noise, consists of jet mixing noise (subscript J) and internally-generated noise (subscript I). The jet mixing noise is assumed to be uncorrelated with the internally-generated noise, so that

$$OASPL = 10 \log \left(10^{OASPL_J/10} + 10^{OASPL_I/10}\right) \quad (1)$$

The following sections describe the methods used herein to compute $OASPL_I$ and $OASPL_J$ and compare the computed values with measured values.

Internally-Generated Noise

The internally-generated noise from a jet engine arises from many sources, such as combustion noise, turbomachinery noise and flow noise.

In the present analysis the acoustics of these sources is lumped, and the predictions are based on measured engine data. Although the internally-generated noise is not directly a function of jet velocity, both noise and jet velocity are unique functions of the engine power for a given engine at standard conditions. Therefore, the internally-generated noise can be mapped as a function of jet velocity, V_j, along the engine operating line for a specific engine at standard conditions. By examining the data for various engines, typical relations can be established.

Variation of $OASPL_I$ with jet velocity. - A representative comparison of static noise data for turbojet engines and model jet nozzles is shown in figure 2 (data of ref. 13) at an angle $\theta = 120^O$ where internally-generated exhaust noise is generally at or near its peak level (refs. 12, 15 and 19). The data shown are corrected for nozzle area, A_j, and source-to-observer distance, R, as well as for the effects of jet density on jet noise (as discussed in a later section). As is typical of engine data, the engine noise levels are well above model jet noise at low V_j, but at higher V_j the engine noise levels agree with those of the model jets. From these data, the non-jet noise, assumed to be internally generated, can be obtained by antilogarithmically subtracting the jet noise (model curve) from the engine data. The resulting normalized noise levels are plotted as a function of the jet velocity parameter, $\log (V_j/c_a)$, in figure 3, for both the Olympus 301 and Viper 520 engines. For both engines the noise levels increase with the fifth power of jet velocity, along the engine operating line, i.e.,

$$OASPL_I - 10 \log \left[\left(\frac{A_j}{R^2}\right)\left(\frac{\rho_j}{\rho_a}\right)^w\right] = K_\theta + 50 \log \left(\frac{V_j}{c_a}\right) \qquad (2)$$

Where K_θ at $\theta = 120^O$ is 146.3 dB for the Olympus 301 and 145.1 dB for the Viper 520. More limited data indicate that K_{120^O} is 146.3 dB for the Olympus 593 and 151 dB for the RB 162. The value chosen as "typical" for further calculations is $K_{120^O} = 146$ dB.

Static OASPL$_I$ directivity. - The variation of OASPL$_I$ referred to that at $\theta = 120^O$ with angle is shown in figure 4 for several engines (refs. 15 and 19) as well as for combustors (ref. 19). The prediction method of references 12 and 15 and that of reference 19 are shown for comparison. Considerable scatter is evident in the experimental data. The prediction methods, being based on different sets of data, are also not in close agreement. The prediction method of reference 19 does not include the full range of angles of interest in this report, so the method of references 12 and 15 is used in these calculations. The sensitivity of these calculations to the static directivity chosen will be further discussed in a later section.

Effect of flight on directivity. - When an acoustic source is in motion its radiation efficiency is altered. Ahead of the moving source, the radiation efficiency is increased, and behind the moving source the radiation efficiency is decreased, while at 90° from the axis of the moving source there is no effect. These effects result from source motion relative to both the observer (kinematic effect) and the propagation medium (dynamic effect).

The effect of source motion relative to the observer is analogous to the well-known Doppler frequency shift. Additionally, the sound intensity is amplified by the Doppler factor, $(1 - M_o \cos \theta)^{-1}$. The effect of source motion relative to the medium on sound intensity may be approximated by the Doppler factor raised to a power dependent on the type of source. Thus, the combined kinematic and dynamic effects may be written in the form,

$$OASPL_F - OASPL_S = -10 \log (1 - M_o \cos \theta)^m \tag{3}$$

In this paper, the assumption $m = 4$ is made. This value of m is consistent with the theory of Morse and Ingard (ref. 16) for a moving monopole and with the theory of Lighthill (ref. 17) for a moving dipole. This formulation, with $m = 4$, has been suggested by Dorsch (ref. 18) for

jet-flap interaction noise, where the noise source moves with the air-plane, as is the case for internally-generated noise. It should be noted, however, that Lighthill (ref. 17) suggests $m = 2$ for a moving monopole; and internally-generated noise may well consist of both monopole (combustion) and dipole (flow-surface interaction) noises. The internally-generated noise flyover directivity used herein is shown in figure 5 for static conditions and for flight Mach numbers M_o of 0.24 and 0.35.

Jet Mixing Noise

Jet mixing noise, both static and in flight, is predicted using the NASA interim prediction method for jet noise (ref. 9). Shock noise is assumed to be absent.

Variation of $OASPL_J$ with jet velocity. - The normalized overall sound pressure level at $\theta = 90^\circ$ for shock-free circular jets, given by $OASPL_J -10 \log \left[(A_j/R^2) (\rho_j/\rho_a)^w \right]$, is plotted as a function of the jet velocity parameter, V_j/c_a, in figure 6 (from ref. 9, results at ISA ambient conditions). The ambient temperature data are for jets ranging from 5.08- to 15.2-cm in diameter (refs. 20 to 22). The hot jet data are for a 38.1-cm-diameter nozzle at temperatures from 700 to 1588 K (refs. 23 and 24). Prediction curves from references 15 and 25 are also shown. Ahuja's prediction for ambient-temperature jets (ref. 25) is in good agreement with the data of figure 6, but is applicable only for $\rho_j \approx \rho_a$ and $V_j \leq c_a$, whereas the prediction of Dunn and Peart (ref. 15) predicts values somewhat lower than the data. The prediction equation chosen in reference 9 (for ISA ambient conditions) and used herein is given by

$$OASPL_J -10 \log \left[\left(\frac{A_j}{R^2}\right)\left(\frac{\rho_j}{\rho_a}\right)^w \right] = 141 + 10 \log \left[\frac{(V_j/c_a)^{7.5}}{1 + 0.01(V_j/c_a)^{4.5}} \right]$$

$$(4)$$

Static OASPL_J directivity. - The jet noise directivity used in this report is an empirical modification of the theoretical result obtained by Goldstein and Howes (ref. 26) for subsonic jets. Goldstein and Howes (ref. 26) found that $\text{OASPL}_J \propto 10 \log (1 + M_c \cos \theta)^{-3}$, where M_c is the source (eddy) convection velocity. These calculations use $M_c = 0.62$ (V_j/c_a), as in reference 9. For values of $M_c \geq 1$, this simple directivity term becomes unbounded at some angles, which is not realistic. To eliminate this singularity, the directivity term of reference 26 was modified in reference 9 to $10 \log \left[1 + M_c \left(1 + M_c^5 \right)^{-1/5} \cos \theta \right]^{-3}$. The effects of refraction are included empirically by a directivity correction factor $F(\theta')$, where $\theta' = \theta (V_j/c_a)^{0.1}$; $F(\theta')$ is given as a function of θ' in figure 7. The complete jet-mixing noise directivity relation is then given as follows:

$$\text{OASPL}_{J,\theta} - \text{OASPL}_{J,90°} = -30 \log \left[1 + M_c \left(1 + M_c^5 \right)^{-1/5} \cos \theta \right] + F(\theta') \tag{5}$$

Effects of flight. - It has been observed in model simulated-flight tests (e.g., refs. 5-8) that forward velocity reduces jet noise at constant jet velocity. Similar reductions were found in early comparisons of aircraft flyover noise data with static data (e.g., refs. 27-30), although it should be emphasized that these studies considered primarily the peak noise. To correlate the effects of flight on jet noise, the effects of forward velocity were considered in two parts in reference 9:

(a) The effect of the external flow field around the nozzle on noise source strength,

(b) The effect of source motion relative to the stationary propagation medium and the stationary observer.

The source strength effect should be observable at $\theta = 90°$ in both flight and simulated-flight tests. Based largely on the results of reference 5, the following relation for the effect of flight on the jet noise at $\theta = 90°$ was obtained in reference 9 and is used herein:

$$\Delta \text{OASPL}_{J,90^{\circ}} = 10 \log \left\{ \left(1 - \frac{V_o}{V_j}\right)^{5.625} \frac{1 + 0.01 \, (V_j/c_a)^{4.5}}{1 + 0.01 \left[(V_j/c_a)(1 - V_o/V_j)^{3/4}\right]^{4.5}} \right\}$$

$$+ 10 \, (w_F - w_S) \log (\rho_j/\rho_a) \tag{6}$$

As in reference 9, the density exponent is assumed to be a function of the effective velocity term $V_j (1 - V_o/V_j)^{3/4}$, as follows:

$$w = \frac{3 \left[(V_j/c_a)(1 - V_o/V_j)^{3/4}\right]^{3.5}}{0.60 + \left[(V_j/c_a)(1 - V_o/V_j)^{3/4}\right]^{3.5}} - 1 \tag{7}$$

This relationship (eq. (7)) does not differ significantly from that used in reference 13 and in the proposed revision to reference 1. It should be noted that the effect of flight or simulated flight on the density exponent has not been evaluated.

The dynamic effect is estimated, as in reference 9, by assuming that the convection Mach number is related to the relative velocity by the following:

$$M_c = 0.62 \, (V_j - V_o)/c_a \tag{8}$$

The correction factor $F(\theta')$ (fig. 7) is assumed to be unaffected by flight. The total effect of flight is then given by

$$\Delta \text{OASPL}_{J,\theta} = \Delta \text{OASPL}_{J,90^{\circ}} - 30 \log \left[\frac{1 + M_{c,F} \left(1 + M_{c,F}^5\right)^{-1/5} \cos \theta}{1 + M_{c,S} \left(1 + M_{c,S}^5\right)^{-1/5} \cos \theta}\right] \tag{9}$$

Comparison of Static Engine Data with Prediction

The noise for a turbojet engine is predicted by summing (eq. (1)) the jet mixing noise and the internally generated noise. The internally-generated noise is calculated from equation (2) and figure 5, while the jet noise is computed from equations (4), (5), (7), and (8) and figure 7. A comparison of the results calculated by these methods with static noise data for turbojet engines is shown in figure 8. The engine data shown (from ref. 13) are corrected for nozzle area A_j, source-to-observer distance R, and jet density. Since some of these data were used in developing the internally-generated noise prediction, it is not surprising that good agreement is seen at low jet velocity. The agreement at high jet velocities confirms that the jet noise prediction is reasonably accurate, at least for static conditions.

Sensitivity of Results to Prediction Methods

In this section the sensitivity of the calculated results to specific elements of the prediction method is considered. In particular different assumptions are tested on the convective amplification and static directivity of the internally-generated noise. Changes in the jet noise prediction method are not considered, although the exact formulation of the effects of flight on jet noise remains to be resolved. The main issue is whether or not the observed increase in noise for a range of angles in flight (e.g., fig. 1) is due to jet noise. (It will be shown in a later section that these results may be due to internally-generated noise.)

The level of internally-generated noise relative to jet mixing noise is, of course, an important factor. If an engine radiated only very low internally-generated noise, either due to less noise generation or tail-pipe acoustic treatment, a point could be reached where the jet noise would be clearly dominant even in flight, and the in-flight noise levels would be below static levels for all angles.

The most critical element in obtaining the cross-over between static and flight directivities is the internally-generated noise convective

amplification (eq. (3)). If this effect were absent no cross-over would be obser red. Reference 15 suggests $m = 2$ in equation (3) instead of $m = 4$ as suggested herein. Computations for these two values of m were made for $V_j/c_a = 1.00$, $M_o = 0.24$ and $(\rho_j/\rho_a) = 0.3$. The results of this change are shown in figure 9(a) where the static and in-flight noise directivities are plotted. The solid curve represents the in-flight noise with $m = 4$, and the dot-dash curve represents the in-flight noise with $m = 2$. For the weaker convective amplification ($m = 2$) the curves still cross, but at smaller values of θ.

The issue of the static directivity of internally-generated noise is not fully resolved, as shown in figure 4. Reference 19 presents a directivity differing from that of references 12 and 15 (used herein). A comparison of the effects of using the different directivity relations is shown in figure 9(b), which presents the in-flight directivity holding the OASPL at $\theta = 120^{\circ}$ constant. There is a significant effect even on the static directivity. This again illustrates that improved prediction methods are needed for the internally-generated noise directivity, as was apparent in the discussion of figure 4. The directivity plot of reference 19 does not extend to low enough angles to determine whether the static and in-flight directivity curves cross.

The combined effects of both changes, static directivity and convective amplification, are shown in figure 9(c). The results do not differ appreciably from figure 9(b), indicating that both the convective amplification and the static directivity of internally-generated noise are sensitive factors in determining the jet engine flight noise directivity. It is believed, therefore, that although there are some uncertainties involved, particularly in the directivity of the internally-generated noise, the prediction methods used herein are realistic within the current state-of-the-art in aircraft noise prediction.

RESULTS AND DISCUSSION

It has been established that the prediction methods agree well with measured static noise data for several turbojet engines over a wide range

of jet velocity. Now these prediction methods will be used to evaluate flight effects on engine exhaust noise by considering the combined contributions of jet-mixing and internally-generated noises.

General

In order to illustrate the effects of flight on jet engine exhaust noise, the following typical case is chosen as an example: a single-engine airplane with $V_j/c_a = 1.8$, $\rho_j/\rho_a = 0.3$, and $M_o = 0.35$. The results of the prediction of the separate jet-mixing and internally-generated noises, as well as their sum, are shown as a function of angle in figure 10, for both the static and in-flight cases. Considering first the static case (fig. 10(a)), it can be seen that the jet noise is dominant at all angles. The total noise, obtained by addition of internally-generated and jet-mixing noises, differs very little from the jet noise, and in an experiment could easily be interpreted as being pure jet noise.

In flight (fig. 10(b)), the jet noise is reduced at all angles, while the internally-generated noise is increased for $\theta < 90^o$ and decreased for $\theta > 90^o$. Thus, in flight the internally-generated noise is dominant for $\theta < 95^o$. It can then be seen that the apparent dominance of jet noise statically does not indicate that at the sar) jet velocity or engine power, jet noise will be dominant in flight, as has often been assumed (e.g., ref. 11). The total noise levels statically and in flight are compared in figure 10(c). The in-flight noise exceeds the static noise for $\theta < 60^o$; this is quite similar to some of the recent flight data (e.g., refs. 10-11). It is apparent then that to achieve the full in-flight reductions typical of jet noise, internally-generated noises must be significantly reduced below present measured values, even for relatively quiet turbofan engines, as was suggested in reference 31.

Flight Effects for Subsonic-Cruise Aircraft

The effect of flight on jet engine exhaust noise is estimated for three jet velocities in the range of interest for subsonic-cruise aircraft, at a flight Mach number of 0.24 (with appropriate values of ρ_j/ρ_a). Two of these conditions (V_j/c_a, 1.00 and 1.88) also correspond to some of the experiments reported in reference 10 and shown herein in figure 1. The total jet engine exhaust noise, both statically and in flight, for these conditions is shown in figure 11. The predicted results have many similarities to the experimental data, indicating a cross-over of the static and flight directivities. However, the calculated curves cross in the vicinity of $\theta = 70^O$ while the experimental curves cross at $\theta > 90^O$ (fig. 1). It is of interest to note that the suppression of peak OASPL with flight decreases with increasing V_j/c_a at constant M_o.

A meaningful comparison of flight data with the prediction must consider the possible sources of inaccuracies or scatter in the flight data. The primary sources of scatter are a lack of knowledge of the precise aircraft position and attitude and the short data sample time. Because of the motion of the airplane during the finite data sample time, each data point represents the average over a range of angles rather than a precise angle. Also, because of the short sample time, the acoustic spectra are subject to scatter, especially at the low frequencies characteristic of jet-mixing and internally-generated noises. Thus, increasing the sample time minimizes the scatter in the noise data but increases the angular imprecision. There would also be errors due to the measurement of airplane velocity, jet velocity and jet density, as well as the effects of ground reflection, atmospheric absorption, and atmospheric inhomogeneities.

Taking into account the effects of the angular imprecision and allowing for a ±1 dB scatter due to the other reasons mentioned in the preceding paragraph, the data of reference 10 for a turbojet engine are compared with the prediction method used herein in figure 12, for $V_j/c_a = 1.00$. Insufficient data are available in reference 10 to allow direct comparisons,

but relative effects can be compared by matching the predicted and measured static noise levels at $\theta = 120^O$, where the accuracy of the prediction methods has been demonstrated (in fig. 8). As can be seen in figure 12(b), the flight data are subject to potentially large errors. Considering the experimental inaccuracies, the flight data do not disagree much with the prediction. However, the agreement in the static case is not so good, particularly at $\theta < 100^O$ (fig. 12(a)). The prediction indicates that in the static case, the internally-generated noise is dominant for this angular range, so this problem appears to be a result of net correctly accounting for the internally-generated noise directivity. If it is assumed that the static experimental data are purely internally-generated noise for $\theta = 120^O$, the flight effects can be estimated from equation (3). Such a correction applied to the measured static data (for $\theta < 120^O$) would be within the error band of the experimental flight data.

Flight Effects for Supersonic-Cruise Aircraft

The effect of flight on jet engine exhaust noise is estimated for three jet velocities in the range of interest for supersonic-cruise aircraft, at a flight Mach number of 0.35 (with appropriate values of ρ_j/ρ_a). The total jet engine exhaust noise, both statically and in flight, for these conditions is shown in figure 13. The angle at which jet-mixing and internally-generated noises are equal, which only occurs in flight, is also indicated. For larger θ jet-mixing noise is dominant, and for smaller θ internally-generated noise is dominant.

Even at these high jet velocities (~600 to 1000 m/sec), the prediction indicates that the static and flight directivities cross. This crossover occurs at $\theta \approx 60^O$, somewhat lower than for the subsonic-cruise case (fig. 11). Again, as in figure 11, the suppression of the peak OASPL with flight decreases with increasing V_j at constant M_O. Not only does the quantity $(1 - V_O/V_j)$ approach unity with increasing V_j, but the slope of the $OASPL_J$ against $\log (V_j/c_a)$ curve is less than at low velocity.

These results indicate that the reduction of noise at constant V_j in flight is considerably less than would be estimated assuming the in-flight noise at each angle is equal to the static noise at a jet velocity equal to $V_j - V_o$, as was assumed for early prediction methods such as reference 1. This is especially true when the effective perceived noise level and noise footprint area are considered, since they are affected by the fact that the noise level remains close to its peak value over a wider angular range.

CONCLUSIONS

This paper demonstrates that some of the anomalous observations of recent flight tests can be reconciled largely on the basis of the combination of jet-mixing noise and internally-generated noise. The anomaly exhibited by the flight data is that the noise is greater in flight than statically over a large range of angles. The prediction methods used herein yield similar results. These results cover a wide range of jet velocity, even including the range of interest for supersonic-cruise aircraft. However, the comparison of the predicted and measured flight effects is somewhat obscured by the inaccuracies of the flight noise measurements and also by the uncertainties in the prediction methods. The predicted results also indicate that even though jet noise may appear to be dominant in static tests, in flight at the same jet velocity or engine power the internally-generated noise may be dominant. For many engines, to achieve the full in-flight reductions typical of jet noise, internally-generated noises must be significantly reduced below present measured values.

APPENDIX - SYMBOLS

A_j full-expanded jet area, m^2

c_a ambient sonic velocity, m/sec

$F(\theta')$ jet noise directivity correction (fig. 7), dB re 20 $\mu N/m^2$

K_θ constant in internally-generated noise prediction, dB re 20 $\mu N/m^2$

L perpendicular distance from observer to flight path, m

m exponent in dynamic-effect relation (eq. (3)), dimensionless

M_c convection Mach number, $0.62\, V_j/c_a$, dimensionless

M_o flight Mach number, V_o/c_a, dimensionless

n relative velocity exponent, dimensionless

OASPL   overall sound pressure level, dB re 20 $\mu N/m^2$

Δ OASPL   change in OASPL with flight, $OASPL_F - OASPL_S$, dB

R source-to-observer distance, m

V_j jet velocity (isentropic, fully expanded), m/sec

V_o airplane velocity, m/sec

w density ratio exponent, dimensionless

ρ_j fully-expanded jet density, kg/m^3

ρ_a ambient density, kg/m^3

θ polar angle from flight path (fig. 1), deg

θ' effective angle, $\theta\, (V_j/c_a)^{0.1}$, deg

Subscripts:

F   flight

I   internally generated

J   jet mixing

S   static

θ evaluated at θ

90° evaluated at $\theta = 90^o$

120° evaluated at $\theta = 120^o$

REFERENCES

1. Society of Automotive Engineers, (1965). "Jet Noise Prediction," SAE Aerospace Information Rept. 876.

2. Ffowcs Williams, J. E., (1963). "The Noise from Turbulence Convected at High Speed," Phil. Trans. Roy. Soc. (London) 255, 469-503.

3. Lighthill, M. J., (1952). "On Sound Generated Aerodynamically. I. General Theory," Proc. Roy. Soc., (London) 211, 564-587.

4. Lighthill, M. J., (1954). "On Sound Generated Aerodynamically. II. Turbulence as a Source of Sound," Proc. Roy. Soc., (London) 222, 1-32.

5. von Glahn, U. H., Groesbeck, D. E., and Goodykoontz, J. H., (1973). "Velocity Decay and Acoustic Characteristics of Various Nozzle Geometries with Forward Velocity," AIAA Paper 73-629.

6. Packman, A. B., Ng, K. W., and Paterson, R. W., (1975). "Effects of Simulated Forward Flight on Subsonic Jet Exhaust Noise," AIAA Paper 75-869.

7. Tanna, H. K.; Tester, B. J.; and Morris, P. J.: The Effects of Motion on Jet Exhaust Noise from Aircraft. Proposed Contractor Report NASA (for contract NAS3-18540), 1975.

8. Cocking, B. J., and Bryce, W. D., (1975). "Subsonic Jet Noise in Flight Based on Some Recent Wind-Tunnel Results," AIAA Paper 75-462.

9. Stone, J. R., (1974). "Interim Prediction Method for Jet Noise," NASA TM X-71618.

10. Brooks, J. R., and Woodrow, R. J., (1975). "The Effects of Forward Speed on a Number of Turbojet Exhaust Silencers," AIAA Paper 75-506.

11. Bushell, K. W., (1975). "Measurement and Prediction of Jet Noise in Flight," AIAA Paper 75-461.

12. Huff, R. G., Clark, B. J., and Dorsch, R. G., (1974). "Interim Prediction Method for Low Frequency Core Engine Noise," NASA TM X-71627.

13. Response to Notice of Proposed Rule Making for the Control of the Noise of Civil Supersonic Airplanes (Docket No. 10494; Notice No. 75-15). Annex 2: Jet Exhaust Silencer Evaluation. An Appraisal of Model and Full Scale Noise Data with Particular Reference to Forward Speed Effects and Simulation. GML/JDV/47091, Rolls-Royce Ltd. (Bristol Engine Div.), 1975.

14. von Glahn, U., and Goodykoontz, J., (1973). "Forward Velocity Effects on Jet Noise with Dominant Internal Noise Source," paper presented at 86th Meeting of the Acoust. Soc. Am., Los Angeles, Calif., Paper 25.

15. Dunn, D. G., and Peart, N. A., (1973). "Aircraft Noise Source and Contour Estimation," Boeing Commercial Airplane Co. Rept. D6-60233; also NASA CR-114649.

16. Morse, P. M., and Ingard, K. U., (1968). Theoretical Acoustics (McGraw-Hill, New York).

17. Lighthill, M. J., (1962). "The Bakerian Lecture, 1961. Sound Generated Aerodynamically," Proc. Roy. Soc. (London), A267, 147-182.

18. Dorsch, R. G., (1974). "Externally Blown Flap Noise Research," SAE Paper 740468.

19. Motsinger, R. E., and Emmerling, J. J., (1975). "Review of Theory and Methods for Combustion Noise Prediction," AIAA Paper 75-541.

20. Olsen, W. A., Gutierrez, O. A., and Dorsch, R. G., (1973). "The Effect of Nozzle Inlet Shape, Lip Thickness, and Exit Shape and Size on Jet Noise," AIAA Paper 73-187.

21. Burrin, R. H., Dean, P. D., and Tanna, H. K., (1973). "A New Anechoic Facility for Supersonic Hot Jet Noise Research at Lockheed-Georgia," paper presented at 86th Meeting of the Acoust. Soc. Am., Los Angeles, Cal., Paper H9.

22. Karchmer, A. M., Dorsch, R. G., and Friedman, R., (1974). "Acoustic Tests of a 15.2-Centimeter-Diameter Potential Flow Nozzle," NASA TM X-2980.

23. von Glahn, U. H., (1972). "Correlation of Total Sound Power and Peak Sideline OASPL from Jet Exhausts," AIAA Paper 72-643.

24. von Glahn, U. H., et al. (1972). "Jet Noise," Aircraft Engine Noise Reduction, NASA SP-311, pp. 103-138.

25. Ahuja, K. K., (1973). "Correlation and Prediction of Jet Noise," J. Sound Vibration 29, 155-168.

26. Goldstein, M. E., and Howes, W. L., (1973), "New Aspects of Subsonic Aerodynamic Noise Theory," NASA TN D-7158.

27. Burley, R. R., Karabinus, R. J., and Freedman, R. J., (1973). "Flight Investigation of Acoustic and Thrust Characteristics of Several Exhaust Nozzles Installed on Underwing Nacelles on an F106 Airplane," NASA TM X-2854.

28. Burley, R. R., and Karabinus, R. J., (1973). "Flyover and Static Tests to Investigate External Flow Effects on Jet Noise for Non-Suppressor and Suppressor Exhaust Nozzles," AIAA Paper 73-190.

29. Brausch, J. F., (1972). "Flight Velocity Influence of Jet Noise of Conical Ejector, Annular Plug and Segmented Suppressor Nozzles," General Electric Co.; Also NASA CR-120961.

30. Coles, W. D., Mihaloew, J. A., and Swann, W. H., (1961). "Ground and In-Flight Acoustic and Performance Characteristics of Jet-Aircraft Exhaust Noise Suppressors," NASA TN D-874.

31. Feiler, C. E., et al., (1975). "I. Propulsion System Noise Reduction. Aeronautical Propulsion," NASA SP-381.
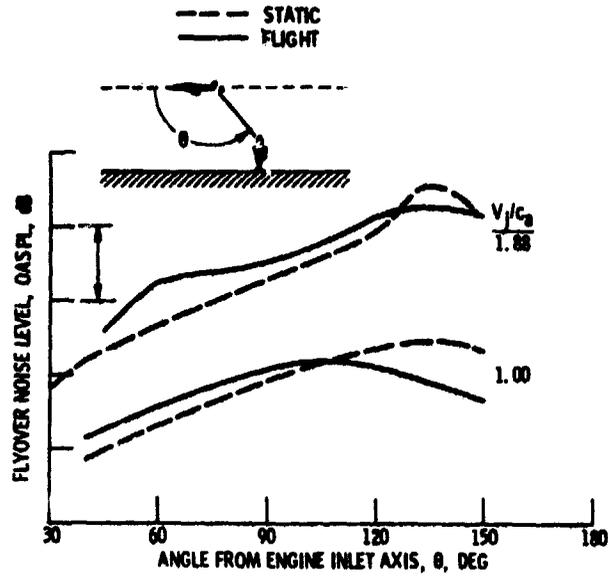
Figure 1. - Flight effects for Viper 601 turbojet engine in HS 125 airplane. Flight Mach number, 0.24. Data of Brooks and Woodrow (ref. 10).
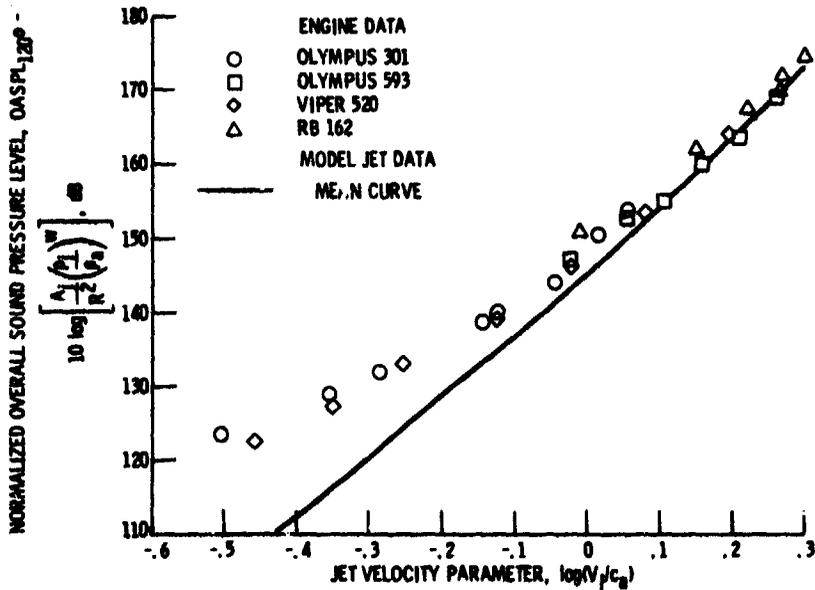

Figure 2. - Comparison of representative static noise data for turbojet engines and model jets at θ = 120° (ref. 13).

PRECEDING PAGE BLANK NOT FILMED
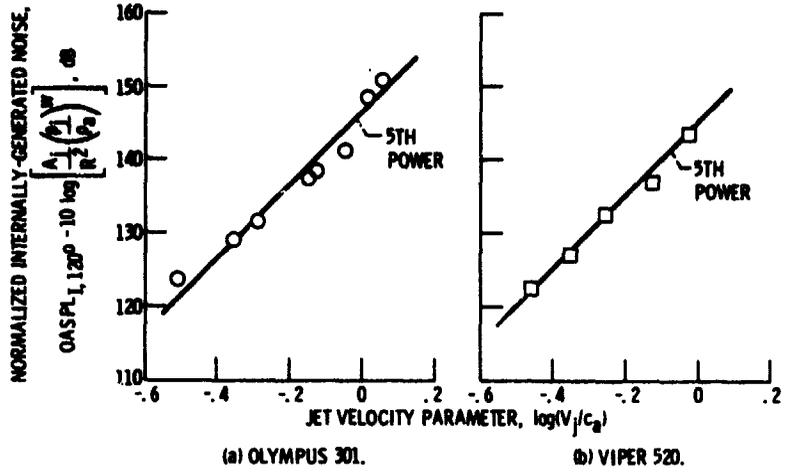
Figure 3. - Internally-generated turbojet engine exhaust noise. Rolls-Royce data (ref. 13) at θ = 120°.

ENGINE DATA	COMBUSTOR DATA	PREDICTION METHODS

● OLYMPUS 301 (REF. 13) ◊ F101 (REF. 19) ——— REFS. 12
■ VIPER 520 (REF. 13) ◖ CF6 (REF. 19) AND 15
◊ TURBOJETS (REF. 15) ――― REF. 19
△ HIGH-BYPASS TURBOFANS (REF. 15)
◣ JT8D-9 (REF. 15)
◗ J85 (REF. 19)
◖ TF34 (REF. 19)
◇ GE4 (REF. 19)
◔ T64 (REF. 19)
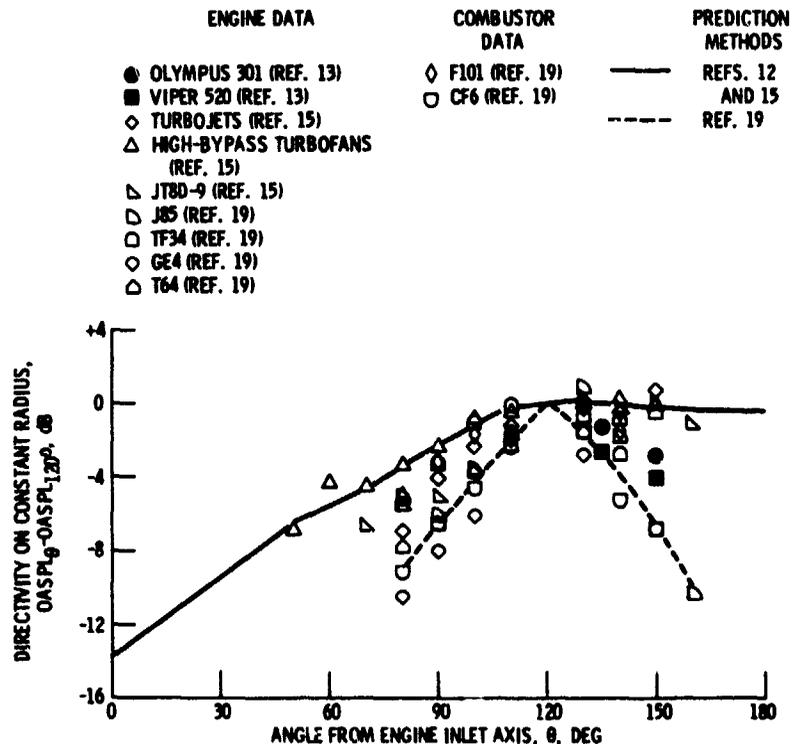
Figure 4. - Internally-generated noise static directivity - comparison of data with prediction methods.

Figure 5. - Flyover directivity for internally-generated jet engine exhaust noise.

EXPERIMENTAL DATA (CORRECTED
TO ISA AMBIENT CONDITIONS)

	NOZZLE DIAMETER, D_e, CM	JET TOTAL TEMPERATURE, T_j, K
○	5.08	~288 (REF. 21)
□	10.2	296 (REF. 20)
◇	15.2	292 (REF. 22)
△	38.1	700 (REFS. 23-24)
◭	38.1	811 (REFS. 23-24)
◮	38.1	922 (REFS. 23-24)
○	38.1	1477 (REFS. 23-24)
◇	38.1	1588 (REFS. 23-24)

——— EQUATION (4), USED HEREIN
(FROM REF. 9)

—-—- PREDICTION OF AHUJA (REF. 25)
FOR $T_j = T_a$

▨▨▨▨ RANGE OF PREDICTION OF DUNN
AND PEART (REF. 15) OVER
T_j RANGE, 300-900 K

Figure 6. - Overall sound pressure level at $\theta = 90^o$ for shock-free circular jets.

Figure 7. - Directivity correction factor as function of effective angle for jet noise prediction of reference 9.
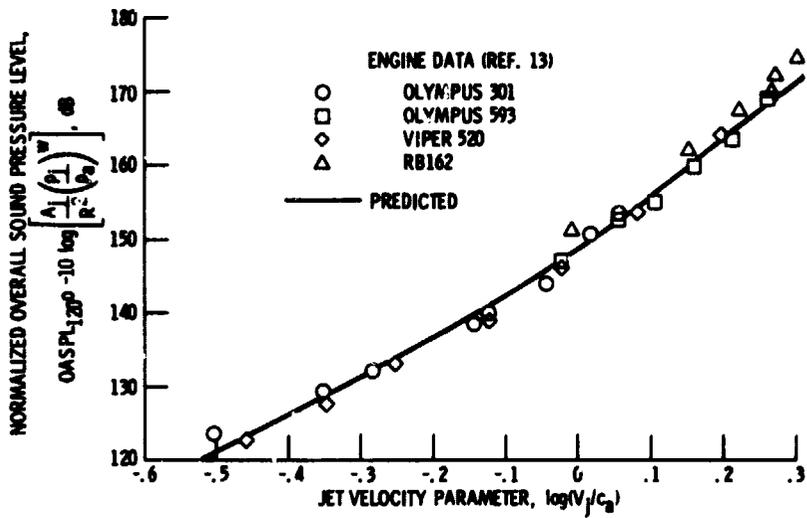
Figure 8. - Comparison of measured static turbojet engine noise data with prediction at θ = 120°.
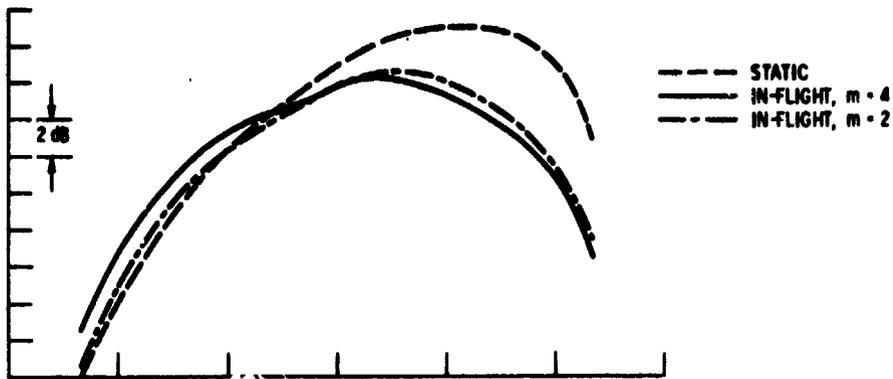
(a) FLIGHT EFFECTS EXPONENT.

(b) STATIC DIRECTIVITY EFFECTS.
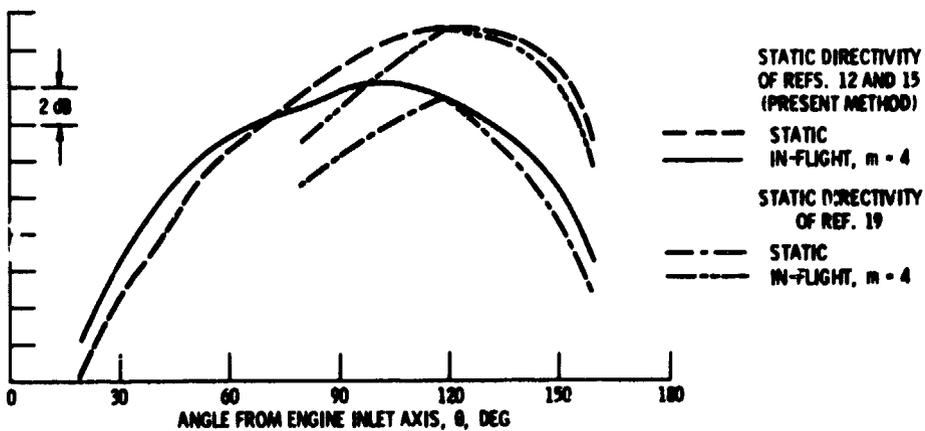
(c) FLIGHT EXPONENT AND STATIC DIRECTIVITY EFFECTS.

Figure 9. – Sensitivity of results to internal noise prediction method elements.
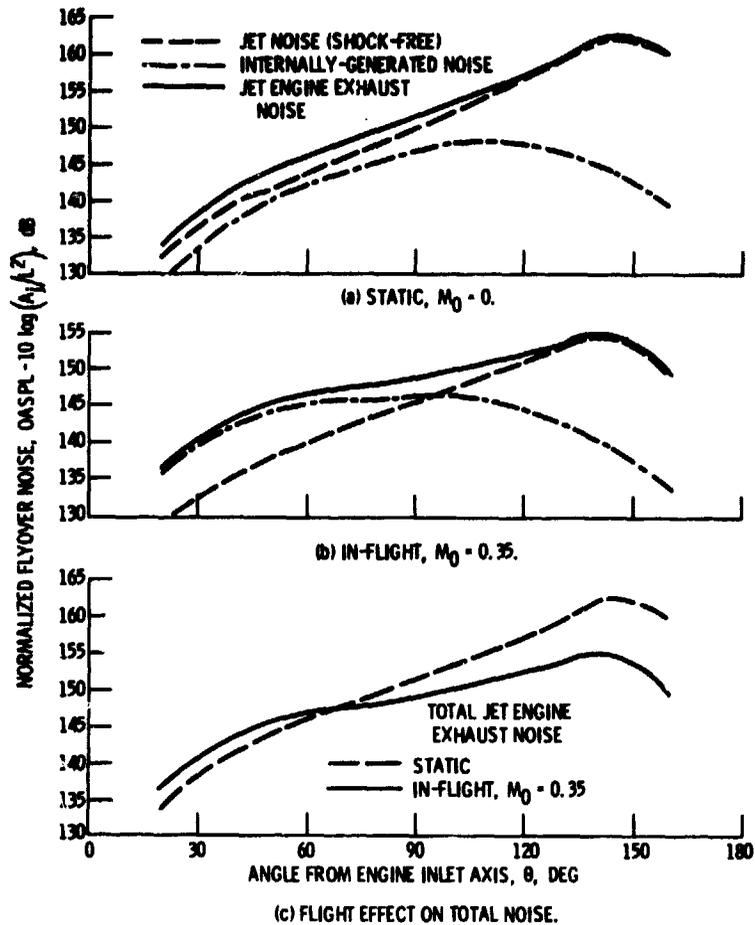
Figure 10. - Synthesis of jet engine exhaust noise directivity; typical jet engine with V_j/c_a = 1.80.
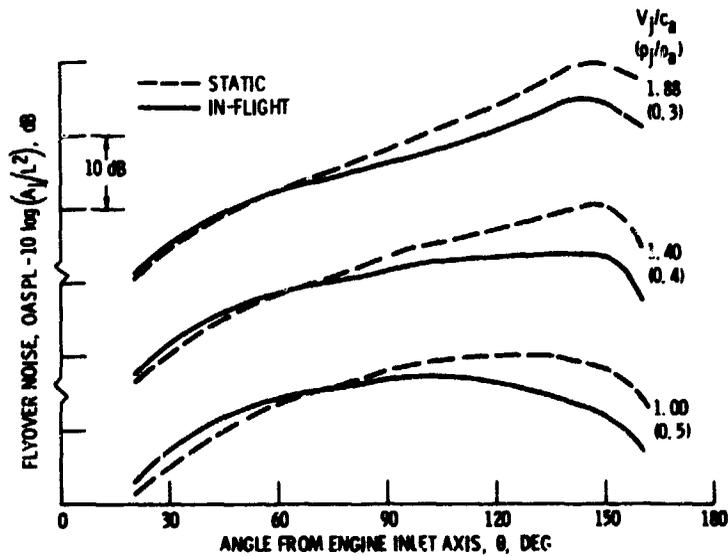
Figure 11. - Synthesis of flight effects on jet engine exhaust noise directivity for subsonic-cruise aircraft. M_0 = 0.24.
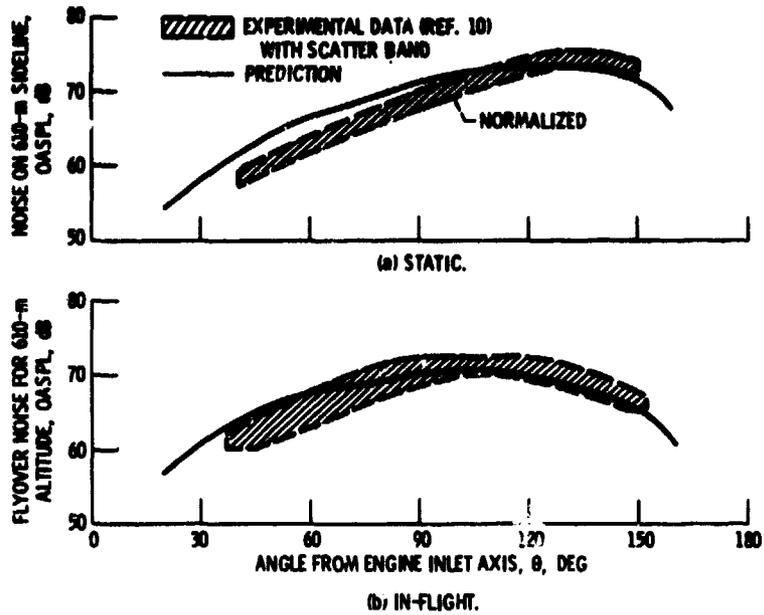
Figure 12. - Comparison of synthesis of flight effects with experimental data for Viper 601 engine in HS125 airplane at $M_0 = 0.24$ and $V_j/c_a = 1.00$.
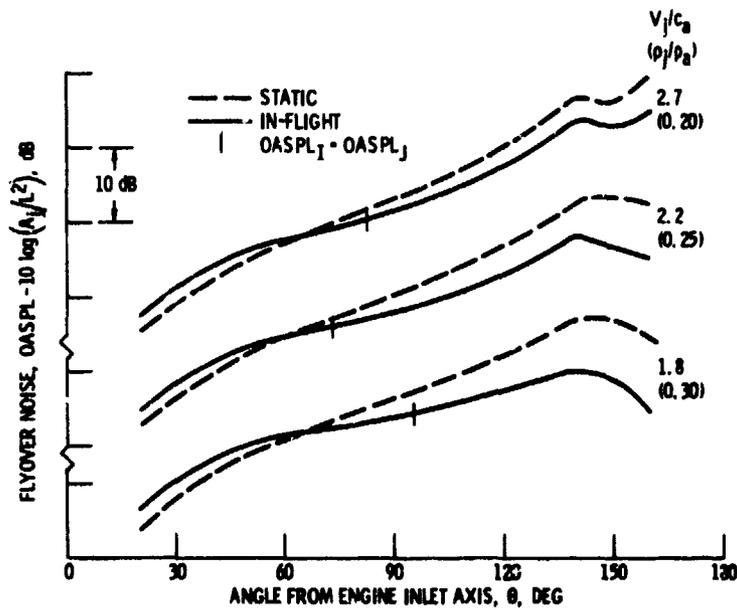

Figure 13. - Synthesis of flight effects on jet engine exhaust noise directivity for supersonic-cruise aircraft - $M_0 = 0.35$.